Spin and Orbital Magnetic Quadrupole Resonances in ^{48}Ca and ^{90}Zr from 180° Electron Scattering

P. von Neumann-Cosel,[1] F. Neumeyer,[1] S. Nishizaki,[2] V. Yu. Ponomarev,[3] C. Rangacharyulu,[4] B. Reitz,[1] A. Richter,[1] G. Schrieder,[1] D. I. Sober,[5] T. Waindzoch,[1,6] and J. Wambach[1]

[1]*Institut für Kernphysik, Technische Universität Darmstadt, D-64289 Darmstadt, Germany*
[2]*Faculty of Humanities and Social Sciences, Iwate University, Ueda 3-18-34, Morioka 020-8550, Japan*
[3]*Bogoliubov Laboratory of Theoretical Physics, Joint Institute for Nuclear Research, Dubna, Russia*
[4]*Department of Physics, University of Saskatchewan, Saskatoon S7N5E2, Canada*
[5]*Department of Physics, Catholic University of America, Washington, DC 20064*
[6]*Institut für Theoretische Physik, Universität Tübingen, D-72076 Tübingen, Germany*

The nuclei ^{48}Ca and ^{90}Zr were investigated in 180° high-resolution inelastic electron scattering for momentum transfers $q \simeq 0.35-0.8$ fm^{-1}. The complete $M2$ strength could be extracted in both nuclei up to excitation energies of about 15 MeV. Second-random-phase approximation calculations successfully describe the strong fragmentation of the experimental strength distributions. Contrary to previous experimental findings, suggesting a severe reduction, the deduced quenching of $M2$ spin matrix elements is comparable to the $M1$ case. A quantitative reproduction of the data requires the presence of appreciable orbital strength which can be interpreted as a torsional elastic vibration ("twist mode").
[S0031-9007(99)08470-7]

Magnetic spin and convection currents of the nucleus, because of their elementary nature, are subjects of continuous experimental and theoretical interest. Magnetic dipole ($M1$) transitions have been studied intensively with emphasis on the problem of "quenching" (i.e., a reduction of the transition strength with respect to the most advanced model predictions) of the spin part. It is now commonly accepted that the quenching results from a combination of coupling to configurations outside the model spaces via the nuclear tensor force and admixtures of the Δ isobar. The latter are small (see [1,2] for some recent work).

Much less is known about magnetic quadrupole ($M2$) excitations whose spin part should also be modified by the mechanisms discussed above. The few available data [3–6] indicate a quenching even stronger than for the $M1$ strength [7]. The spin part of the $M2$ strength is directly related to the $J^{\pi} = 2^{-}$ component of spin-dipole excitations [8,9] observed in hadron scattering experiments whose spin decomposition is a central goal of recent experimental efforts [10]. The amount of quenching and the $M2$-strength distributions in sd- and fp-shell nuclei are also key ingredients for a detailed modeling of the late stages of heavy stars before a supernova collapse [11,12] and for the ν-nucleosynthesis process [13]. Calculations of the $M2$ response in nuclei have been performed in various microscopic approaches [14–18]. Although the centroid of the observed $M2$ strength distribution is roughly reproduced on the random-phase approximation (RPA) level taking into account one particle–one hole ($1p1h$) excitations, the strong fragmentation of the mode can only be described by coupling to the large number of two particle–two hole ($2p2h$) states.

There is, furthermore, a fundamental interest in verifying the possible existence of an orbital $M2$ resonance in spherical nuclei. Such an excitation, predicted within a fluid-dynamic approach for finite Fermi systems [19] and named "twist mode," can be viewed as a rotation of different layers of fluid against each other with a rotational angle proportional to the distance along the axis of rotation. Having no restoring force in an ideal fluid, its experimental observation would be direct proof of the zero sound character of giant resonances in nuclei which can be interpreted as vibrations of an elastic medium, in contrast to the hydrodynamical picture [20]. Backward electron scattering presents the most promising tool to search for such a mode [21–23].

The present work aims at a solution of some of these open questions. We have chosen to study ^{48}Ca and ^{90}Zr as first examples of a systematic investigation of the $M2$ spin quenching as well as to search for experimental indications of the orbital twist mode. Modern developments of second-RPA (SRPA) theories [24] provide a promising tool for a realistic description of the $M2$ strength distributions in medium-mass and heavy nuclei.

Electron scattering at 180° is particularly suited because of the strong suppression of longitudinal excitations including the radiative tail dominated by elastic scattering [25]. Thus, it serves as a filter for transverse excitations. Exceptional features compared to similar previous devices can be achieved [26] at the S-DALINAC by the coupling of the 180° system to a large solid angle, large momentum acceptance spectrometer [27]. For the first time, a 10 MHz pulsed beam originally developed for a free electron laser [28] was employed to distinguish the electrons scattered

off the target from those of background sources (e.g., the Faraday cup or slit systems) by the time-of-flight differences of the detected electrons. With this technique the signal-to-background ratio in the measured spectra could be increased by up to an order of magnitude. Compared to the limited information from previous (e, e') experiments [3–6], these experimental developments permit an extraction of the *entire* $M2$ response over *large* excitation energy regions essential for an answer to the problems raised above.

For the measurements isotopically enriched (>97%) metallic foils ^{48}Ca and ^{90}Zr with target thicknesses of 10.2 mg/cm^2 and 19.8 mg/cm^2, respectively, were used. Spectra were taken at electron energies $E_0 = 42.4$, 66.4, and 82.2 MeV corresponding to momentum transfers $q = 0.38$, 0.62, and 0.78 fm^{-1}. Typical beam currents were 1–3 μA. The energy resolution, dominated by the target thickness, ranged from 50 to 70 keV. The spectrometer settings covered an excitation energy range $E_x = 4$–15 MeV. The upper part of Fig. 1 presents a typical ^{48}Ca(e, e') spectrum taken at $E_0 = 66.4$ MeV. Above 8 MeV it is dominated by transitions to 2^- states. The spin information and reduced transition probabilities were derived from fits of RPA form factors to the experimental data including, where available, results from previous (e, e') experiments [29,30].

At energies $E_x > 11$ MeV the level density of 2^- states in ^{48}Ca becomes very high leading to a considerable fragmentation of the transition strength. Thus, the unfolding procedure of the spectra as a superposition of discrete
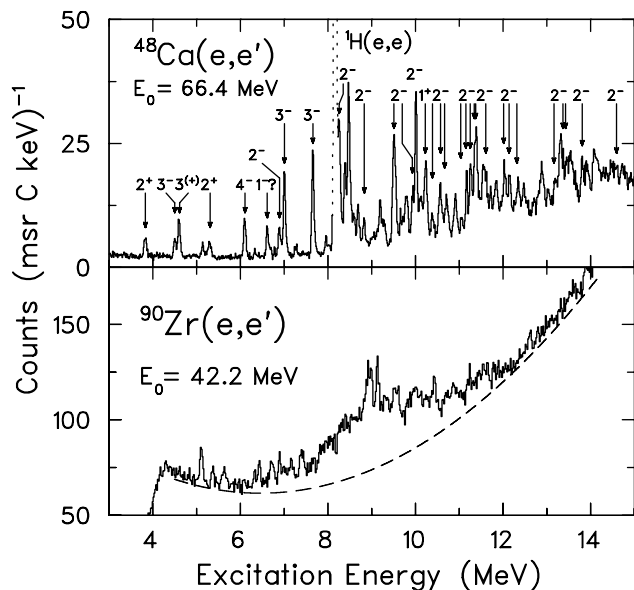
lines is no longer possible. Parts of the $M2$ strength might thus be hidden in the background of the spectra. This problem is even more pronounced in the spectrum of ^{90}Zr displayed in the lower part of Fig. 1. The strong rise of the radiative tail (dashed line) sets in at lower excitation energies, but a prominent resonancelike structure around 9 MeV is clearly visible, which has been identified to be mostly of an $M2$ nature [4,6].

A solution to this problem is provided by a fluctuation analysis technique based upon a statistical treatment, i.e., assuming Wigner-type level spacings and Porter-Thomas intensity distributions (for details, see [31]). To extract the total $B(M2)\uparrow$ strength in the excitation energy region covered by the experiment, an analysis similar to the one in Ref. [32] was performed in the intervals $E_x = 11$–15 MeV (^{48}Ca) and 7–12 MeV (^{90}Zr). At higher energies in ^{90}Zr one probably enters the regime of Ericson fluctuations [33], which precludes application of the above method. The combined $M2$-strength distribution for ^{48}Ca is summarized in the top part of Fig. 2.

Attempts to describe the complex $M2$-strength distributions by RPA calculations fail (independent of details of the residual interaction). One has to invoke the SRPA, which extends the model space to include $2p2h$ excitations on the correlated ground state. Since both mean-field and collisional damping are included, the SRPA is well suited for a description of the fine structure of nuclear modes [20,34]. When evaluated in a basis of RPA states $|\nu\rangle$ the strength function takes the form [24]

$$S_F(E) = -\frac{1}{\pi} \text{Im} \sum_{\nu\nu'} \langle 0|\hat{F}^\dagger|\nu\rangle G_{\nu\nu'}(E) \langle \nu'|\hat{F}|0\rangle, \quad (1)$$

where $\hat{F}$ denotes the operator of the perturbing field. In the case of magnetic excitations, $\hat{F}$ couples to the current
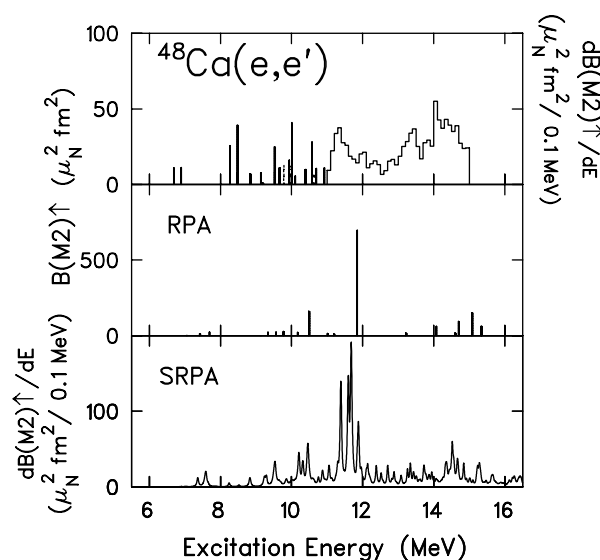

FIG. 1. Upper part: Inelastic electron scattering spectrum of ^{48}Ca taken at $\theta = 180°$ and $E_0 = 66.4$ MeV. The spins and parities of most states are determined from form factor measurements. The dotted line shows electrons elastically scattered off a ^{1}H contamination. Lower part: Spectrum of ^{90}Zr at $E_0 = 42.2$ MeV. The dashed line indicates the background due to the radiative tail.

FIG. 2. Comparison of the $M2$ strength distribution in ^{48}Ca with results of RPA and SRPA calculations described in the text.

operator

$$\hat{\mathbf{j}}(\mathbf{r}) = \sum_{k=1}^{A} \frac{e}{2m_N} [ig_l^{(k)}\{\nabla, \delta(\mathbf{r} - \mathbf{r_k})\}$$
$$+ g_s^{(k)}(\nabla \times \mathbf{s_k})\delta(\mathbf{r} - \mathbf{r_k})], \qquad (2)$$

where $g_l^{(k)}$ and $g_s^{(k)}$ are the orbital and spin g factors of the kth nucleon, respectively. Taking into account distortions of the electron in the static Coulomb field of the nucleus, $\hat{F}$ is then evaluated by convoluting the current (2) with the distorted waves of the incoming and outgoing electron. The Green's function in Eq. (1) is given by

$$G_{\nu\nu'}(E) = [E - E_\nu - \Sigma_{\nu\nu'}(E) + i\eta]^{-1}$$
$$- [E + E_\nu + \Sigma_{\nu\nu'}(-E) - i\eta]^{-1}, \qquad (3)$$

where E_ν are the RPA eigenenergies. The coupling to $2p2h$ excitations results in a complex self-energy $\Sigma_{\nu\nu'} \equiv \Delta_{\nu\nu'} - \frac{i}{2}\Gamma_{\nu\nu'}$. After diagonalization of the residual interaction, $\hat{v}$, in the $2p2h$ subspace it takes the form

$$\Sigma_{\nu\nu'}(E) = \sum_2 \langle\nu|\hat{v}|2\rangle \frac{1}{E - E_2 + i\eta} \langle 2|\hat{v}|\nu'\rangle. \qquad (4)$$

To account for finite energy resolution in the experiment, η in Eq. (4) is taken to be finite (typically 20 keV).

In the calculations presented below, single-particle energies were taken from experiment when available. Otherwise, they (as well as the single-particle wave functions) were obtained from a static Woods-Saxon potential with parameters to optimally reproduce the ground-state properties [35]. All $2p2h$ states up to 28 MeV (^{48}Ca) and 21 MeV (^{90}Zr) were included. As residual interaction we choose the "M3Y" interaction of Ref. [36] which is a finite-range parametrization of the G matrix. As is well known the real part $\Delta_{\nu\nu'}$ of the RPA self-energy is attractive at low excitation energies, mainly because of the dressing of particle and hole lines [20,34]. Since the single-particle energies are obtained from a Woods-Saxon potential or from experiment, such effects are largely taken into account. Among various possibilities for correcting this "double-counting" problem [24], a very satisfactory prescription is to subtract from $\Delta_{\nu\nu'}$ a smooth part $\bar{\Delta}_{\nu\nu'}$ which is obtained using a larger energy averaging parameter, η (200 keV). As a result, the subtracted $\Delta_{\nu\nu'}$ fluctuates around zero, preserving the correct pole structure for the damping of the RPA modes into $2p2h$ states.

The RPA results (middle part of Fig. 2) predict a compact resonance at about 12 MeV in contrast to the strong fragmentation visible in the experimental results. However, if the coupling to $2p2h$ excitations is taken into account in the SRPA calculation, the description is greatly improved (bottom part of Fig. 2). The main structures of the experimental strength distribution with clustering around 10, 12, and 15 MeV can be well reproduced, although the experimental strength is still somewhat more spread out. The situation is similar in ^{90}Zr.

In order to see to what extent the present results exhaust the theoretical $M2$ strengths, it is instructive to plot the energy-weighted running sums as a function of excitation energy (Fig. 3). The hatched areas indicate the experimental uncertainties dominated by the assumptions on the level densities in the fluctuation analysis. The experimental results exhaust 30% (^{48}Ca) and 21% (^{90}Zr), respectively, of the RPA energy-weighted sum rule (EWSR) values given in the caption of Fig. 3. Note that exchange contributions to the EWSR are neglected. Their inclusion would lead to corrections of the order 10% for the M3Y interaction. The dashed lines represent the SRPA results using an effective spin g factor $g_s^{\text{eff}} = 0.64g_s^{\text{free}}$, adjusted to reproduce the $M1$ data in ^{48}Ca [37]. The good agreement with the data shown in Fig. 3 demonstrates that (assuming $g_l^{\text{eff}} = g_l^{\text{free}}$) the spin quenching of $M1$ and $M2$ strengths is very similar.

Finally, we address the possible evidence for an orbital $M2$ mode. At present, arguments can be based only on a decomposition in the SRPA predictions. Figure 4 compares the ^{90}Zr results with the calculated total $B(M2)$ distribution and its separation into spin and orbital contributions. One indeed finds significant orbital strength. The interference pattern leads to a suppression of the total strength at low excitation energies and an enhancement above approximately 7 MeV. Because of the comparable magnitudes of spin and orbital strengths, the constructive interference reaches maximum values in the main bump of the $M2$ resonance around 9 MeV. Thus, the agreement of the SRPA calculations (which would be completely spoiled in the absence of the orbital strength) provides a strong argument for the presence of the twist mode. The properties of the twist mode can be characterized by its
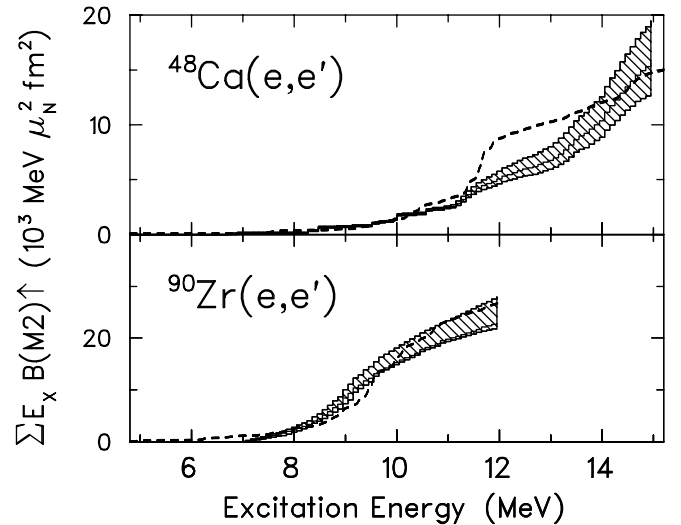

FIG. 3. Running sums of the energy-weighted $B(M2)$ strengths in ^{48}Ca and ^{90}Zr. The RPA-EWSR values are $52.4 \times 10^3 \mu_N^2$ MeV fm^2 (^{48}Ca) and $112.3 \times 10^3 \mu_N^2$ MeV fm^2 (^{90}Zr), respectively. The dashed lines are SRPA calculations with an effective spin g factor $g_s^{\text{eff}} = 0.64g_s^{\text{free}}$ which was adjusted to reproduce the $M1$ strength in ^{48}Ca.
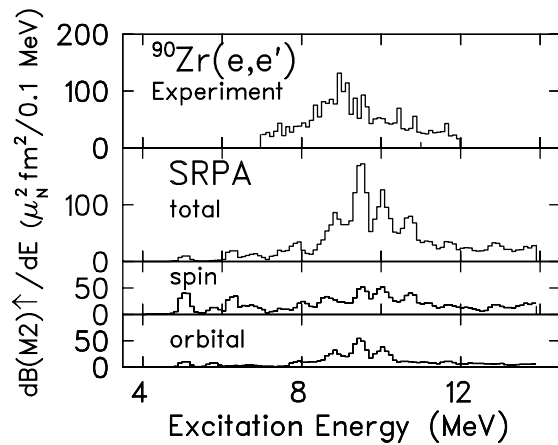
FIG. 4. Comparison of the experimental $B(M2)$ distribution in ^{90}Zr with SRPA results for the total strength and the decomposition into spin and orbital parts.

total strength and the mean energy $\bar{E}$ which is related to the nuclear shear modulus μ [22,38]. For ^{90}Zr one finds from the present work $B(M2)_l\uparrow = 780\mu_N^2$ fm^2, $\bar{E} = 9.7$ MeV in reasonable agreement with the original prediction [19] of $B(M2)_l\uparrow = 830\mu_N^2$ fm^2, $\bar{E} = 9.0$ MeV. The resulting shear moduli expressed in units of the nuclear matter density $\rho_0 = 0.17$ fm^{-3} are $\mu/\rho_0 = 6.3$ MeV (^{48}Ca) and 7.2 MeV (^{90}Zr). This corresponds to 41% (^{48}Ca) and 47% (^{90}Zr), respectively, of the nuclear matter value of 15.34 MeV. The overall reduction and the relative differences in finite nuclei can be understood to arise from surface contributions.

To summarize, we have extracted from 180° electron scattering experiments the complete $M2$ response in ^{48}Ca and ^{90}Zr up to excitation energies of about 15 MeV. The structure of the complex, highly fragmented strength distributions is well accounted for by SRPA calculations. For a quantitative description a reduction of the spin part must be invoked. The degree of quenching is found to be very similar for $M1$ and $M2$ transitions, contrary to earlier claims. The good agreement of the model results with the data depends sensitively on a pronounced constructive spin/orbital interference which provides a strong indication for the presence of the orbital twist mode. Clearly, the latter argument is only indirect and a direct proof (e.g., through the different form factor dependence of spin and orbital parts) must await future experiments. For systematic tests of sum-rule predictions [39–43] it would also be of importance to establish these elementary magnetic quadrupole modes over a wide mass range.

[1] T. Wakasa *et al.,* Phys. Rev. C **55**, 2909 (1997); Phys. Lett. B **426**, 257 (1998).
[2] B. Reitz *et al.,* Phys. Rev. Lett. **82**, 291 (1999).
[3] R. Frey *et al.,* Phys. Lett. **74B**, 45 (1978).
[4] D. Meuer *et al.,* Nucl. Phys. **A349**, 309 (1980).
[5] D. Meuer *et al.,* Phys. Lett. **106B**, 289 (1981).
[6] S. Müller *et al.,* Phys. Lett. **113B**, 362 (1982).
[7] C. Lüttge *et al.,* Nucl. Phys. **A606**, 183 (1996).
[8] F. Osterfeld, Rev. Mod. Phys. **64**, 491 (1992).
[9] F. T. Baker *et al.,* Phys. Rep. **289**, 235 (1997).
[10] *Proceedings of the International Symposium on New Facet of Spin Giant Resonances in Nuclei,* edited by H. Sakai *et al.* (World Scientific, Singapore, 1998).
[11] A. Zaringhalam, Nucl. Phys. **A404**, 599 (1983).
[12] J. Cooperstein and J. Wambach, Nucl. Phys. **A420**, 591 (1984).
[13] S. E. Woosley *et al.,* Astrophys. J. **356**, 272 (1990).
[14] W. Knüpfer *et al.,* Phys. Lett. **77B**, 367 (1978).
[15] V. Yu. Ponomarev *et al.,* Nucl. Phys. **A323**, 446 (1979).
[16] V. Yu. Ponomarev *et al.,* Phys. Lett. **97B**, 4 (1980).
[17] D. Cha and J. Speth, Phys. Rev. C **29**, 636 (1984).
[18] D. Cha *et al.,* Nucl. Phys. **A430**, 321 (1984).
[19] G. Holzwarth and G. Eckart, Z. Phys. A **283**, 219 (1977); Nucl. Phys. **A325**, 1 (1979).
[20] J. Speth and J. Wambach, in *Electric and Magnetic Giant Resonances in Nuclei,* edited by J. Speth (World Scientific, Singapore, 1991), p. 1.
[21] B. Schwesinger, K. Pingel, and G. Holzwarth, Nucl. Phys **A341**, 1 (1982).
[22] B. Schwesinger, Phys. Rev. C **29**, 1475 (1984).
[23] V. Yu. Ponomarev, J. Phys. G **10**, L177 (1984).
[24] S. Drożdż *et al.,* Phys. Rep. **197**, 1 (1990).
[25] L. W. Fagg, Rev. Mod. Phys. **47**, 683 (1975).
[26] C. Lüttge *et al.,* Nucl. Instrum. Methods Phys. Res., Sect. A **366**, 325 (1995).
[27] H. Diesener *et al.,* Phys. Rev. Lett. **72**, 1994 (1994).
[28] A. Richter, Phys. Bl. **54**, 31 (1998).
[29] W. Steffen, Dissertation D17, Technische Hochschule Darmstadt, 1984.
[30] J. E. Wise *et al.,* Phys. Rev. C **31**, 1699 (1985).
[31] P. G. Hansen, B. Jonson, and A. Richter, Nucl. Phys. **A518**, 13 (1990).
[32] J. Enders *et al.,* Phys. Rev. Lett. **79**, 2010 (1997).
[33] T. Ericson, Adv. Phys. **9**, 425 (1960).
[34] J. Wambach, Rep. Prog. Phys. **51**, 989 (1988).
[35] F. Neumeier, Dissertation D17, Technische Universität Darmstadt, 1998.
[36] G. F. Bertsch *et al.,* Nucl. Phys. **A284**, 399 (1977).
[37] W. Steffen *et al.,* Nucl. Phys. **A404**, 413 (1983).
[38] S. Nishizaki and K. Andō, Prog. Theor. Phys. **71**, 1263 (1984).
[39] M. Traini, Phys. Rev. Lett. **41**, 1535 (1978).
[40] T. Suzuki, Phys. Lett. **83B**, 147 (1979).
[41] S. Nishizaki and K. Andō, Prog. Theor. Phys. **63**, 1599 (1980).
[42] E. Lipparini and S. Stringari, Phys. Rep. **175**, 103 (1989).
[43] D. Kurath, Argonne National Laboratory Report No. 97/14, 1997, p. 161.